Publication Year	2022
Acceptance in OA	2025-04-02T09:37:31Z
Title	The expanded, parallel, and monochromatic x-ray beam of BEaTriX: alignment and characterization
Authors	BASSO, Stefano, SALMASO, Bianca, GHIGO, Mauro, SPIGA, Daniele, VECCHI, Gabriele, SIRONI, GIORGIA, COTRONEO, Vincenzo, Conconi, P., Redaelli, E., BIANCO, ANDREA, PARESCHI, Giovanni, TAGLIAFERRI, Gianpiero, Sisana, D., Pelliciari, C., FIORINI, MAURO, INCORVAIA, Salvatore, USLENGHI, Michela, PAOLETTI, Lorenzo, Ferrari, C., Beretta, S., Zappettini, A., del Rio, M. Sanchez. ., Parodi, G., Burwitz, V., Rukdee, S., Hartner, G., Müller, T., SCHMIDT, TOBIAS MARIUS, Langmeier, A., Ferreira, D. D., Massahi, S., Gellert, N. C., Christensen, F., Bavdaz, M., Ferreira, I.
Publisher's version (DOI)	10.1117/12.2629921
Handle	http://hdl.handle.net/20.500.12386/36999
Serie	PROCEEDINGS OF SPIE
Volume	12181

The expanded, parallel and monochromatic X-ray beam of BEaTriX: alignment and characterization

S. Basso[1a], B. Salmaso[a], M. Ghigo[a], D. Spiga[a], G. Vecchi[a], G. Sironi[a], V. Cotroneo[a], P. Conconi[a], E. Redaelli[a], A. Bianco[a], G. Pareschi[a], G. Tagliaferri[a], D. Sisana[b], C. Pelliciari[c], M. Fiorini[d], S. Incorvaia[d], M. Uslenghi[d], L. Paoletti[e], C. Ferrari[f], S. Beretta[f], A. Zappettini[f], M. Sanchez del Rio[g], G. Parodi[h], V. Burwitz[i], S. Rukdee[i], G. Hartner[i], T. Müller[i], T. Schmidt[i], A. Langmeier[i], D.D. Ferreira[l], S. Massahi[l], N.C. Gellert[l], F. Christensen[l], M. Bavdaz[m], I. Ferreira[m]

[a]INAF Astronomical Observatory Brera, Via E. Bianchi 46, 23807 Merate, Lecco (Italy)
[b]Politecnico Milano Bovisa, Via La Masa 34, 20156 Milano (Italy)
[c]IIS Bachelet, Via Stignani 63/65, 20081 Abbiategrasso, Milano (Italy)
[d]INAF-IASF Milano, Via A. Corti 12, 40133 Milano (Italy)
[e]INAF Astronomical Observatory Padova, Vicolo Osservatorio 5, 35122 Padova (Italy)
[f]IMEM-CNR, Parco Area delle Scienze 37/A, 43124 Parma (Italy)
[g]European Synchrotron Radiation Facility, B.P. 220, 38043 Grenoble (France)
[h]BCV Progetti, Via S. Orsola 1, 20123 Milano (Italy)
[i]Max-Planck-Institut für extraterrestrische Physik, Giessenbachstr, 85748 Garching (Germany)
[l]DTU-space, Juliane Maries Vej 30, DK-2100 Copenhagen (Denmark)
[m]ESTEC, European Space Agency, Keplerlaan 1, 2201 AZ Noordwijk (Netherlands)

ABSTRACT

BEaTriX (Beam Expander Testing X-ray) is the compact (18m × 9m) X-ray facility being implemented at INAF for the acceptance tests of the ATHENA Silicon Pore Optics Mirror Modules (MM) working at the two energies of 1.49 and 4.51 keV. It adopts an innovative design based on a collimating mirror and Bragg crystals in proper configuration to provide a large and parallel beam. The 4.51 keV line provides a parallel beam with 170 mm x 60 mm size and it has been calibrated and characterized in term of intensity, uniformity, divergence and stability. This paper traces the path taken for the best-achieved alignment of the different optical components, from the preliminary phases to the final step where the function of merit was obtained directly from the parallel beam itself. The alignment method used a combination of optical and mechanical tools: laser tracker, micro-alignment telescope (MAT), 3D measuring machine (CMM) and self-designed holed plates. The final characterization of the X-ray beam is presented.

Keywords: ATHENA, BEaTriX, X-ray testing, X-ray facility, beam expander, parallel beam, optic alignment, Hartmann plate

1. INTRODUCTION

BEaTriX (Beam Expander Testing X-ray) is the X-ray facility implemented at INAF for the acceptance tests of the ATHENA[1] Silicon Pore Optics Mirror Modules (MM)[2][3] working at the two energies of 1.49 and 4.51 keV. It is a unique facility able to achieve a collimation of the beam within 2 arcsec with a compact (18m × 9m) laboratory without the necessity to place the X-ray source at a distance of hundreds of meters, concept adopted in other facilities for X-ray

[1] corresponding author: stefano.basso@inaf.it; phone +39-02-72320-496; www.brera.inaf.it

Space Telescopes and Instrumentation 2022: Ultraviolet to Gamma Ray, edited by Jan-Willem A. den Herder, Shouleh Nikzad, Kazuhiro Nakazawa, Proc. of SPIE Vol. 12181, 121814D · © 2022 SPIE · 0277-786X · doi: 10.1117/12.2629921

calibration like MPE PANTER (Germany). In the PANTER facility, the X-ray source is placed at a 120m distance from the optic to be tested, obtaining a divergence of 100 arcsec within the typical size of a MM[4]. A reduction of the divergence below 1 arcsec can be achieved using a Zone Plate (ZP) [5], at the specific energy for which it was designed. Anyway, the PANTER facility is very large and the evacuation time is not compatible with the measuring rate foreseen for the MMs (2 MM/day). On the contrary, BEaTriX is a small facility and it is divided into sectors where the vacuum can be broken independently; in particular, the chamber where the MM is mounted can be isolated, leading to 1-2 h time for venting, changing the MM and evacuation.
Another facility used for the alignment and measurements of the MMs is the beam line XPBF 2.0 of PTB[6], at BESSY-II in Berlin. This facility combines a narrow size beam (up to 7.5 × 7.5 mm^2), highly collimated (about 2 arcsec) and with a high photon density (about 10^{13} ph/s), to a precise mechanics, that moves the MM along the beam, providing sub-aperture exposures, that need to be recomposed via software analysis. The process is time consuming, requiring several hours to reconstruct the overall PSF. In BEaTriX, the time needed to acquire the entire PSF is much faster (~30 minutes); moreover effective area measurements are possible within a few percent error.
To create the large parallel and highly monochromatic beam of BEaTriX, an accurate alignment of all the optical components was carried out. This paper describes in detail the alignment process, its theoretical approach and the experimental results in term of intensity, stability, uniformity and divergence. The facility has been characterized and the first light with a MM has been obtained with the operative line at 4,51 keV.

2. DESCRIPTION OF THE BEATRIX FACILITY

The current operative beam line in BEaTriX is at 4.51 keV and the working principle is sketched in Figure 1 [7]-[19].
All the optical components are installed in vacuum chambers ($P<10^{-4}$ mbar) in order to propagate the X-rays from the source to the detector. The divergent beam, coming from the X-ray source, is collimated by a parabolic mirror and monochromated by two channel cut crystals (CCC1 and CCC2) in Si (220). The beam is then diffracted by another crystal in Si (220) named Beam Expander (BE): this last crystal is asymmetrically cut to horizontally expand the beam by about 50 times. By doing so, the BE bends the beam to about 90 degrees. After this moderation, the beam size is 170 mm × 60 mm with a flux of about 60 ph/s/cm^2.
The expanded and parallel beam is then propagated to a separated chamber (MM chamber), where the MM to be tested is installed, and, after being reflected, it is focused at 12m (the Athena focal length). A detailed description of the facility is in Ref. [20].

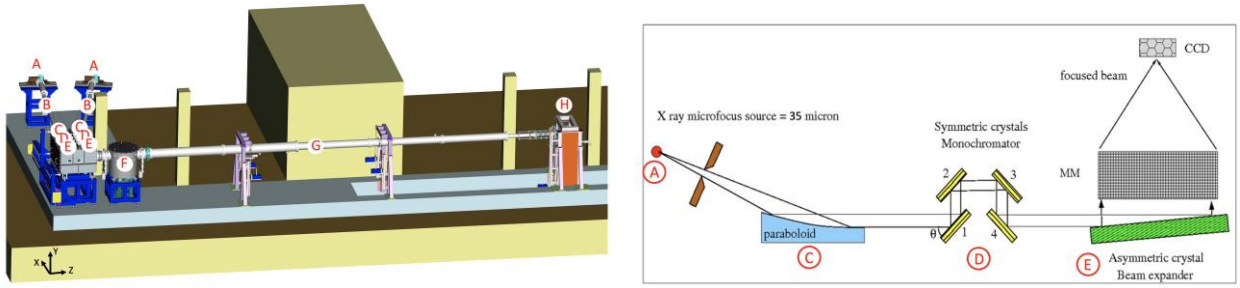

Figure 1. BEaTriX elements: view of position of the components in the facility (left) and optical scheme (right). The BEaTriX coordinate system has the Z axis aligned with the Long Arm, and the Y axis normal to the floor, in accordance to the Athena coordinate system.

3. ALIGNMENT

The correct alignment of the optical components is a key phase to obtain a collimated beam with a uniformity as best as possible with the expected number of photons. The process involved all the components and has been obtained with several measuring instruments and different adopted setup.
The major steps are described in the following flowchart and are further detailed in the next subsections.

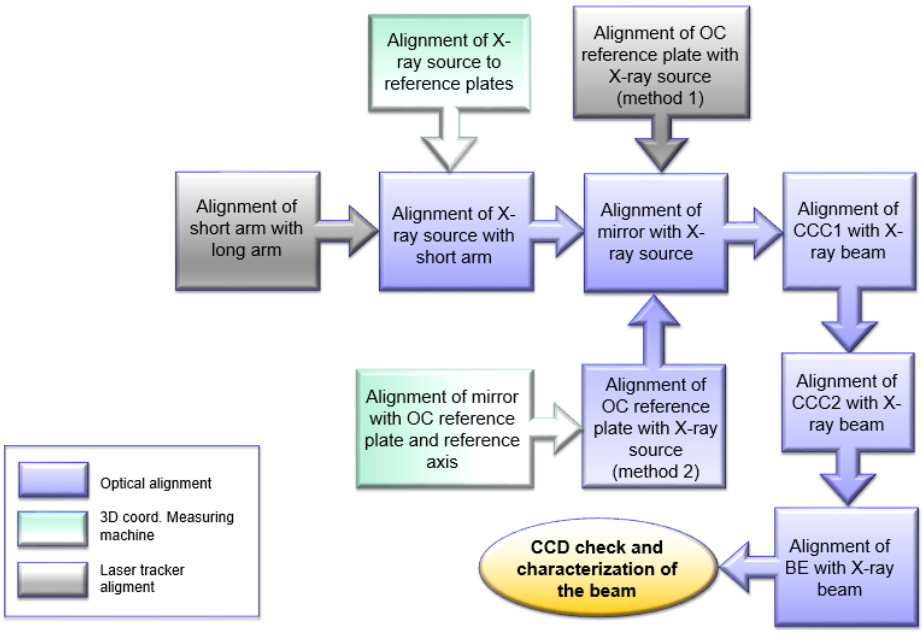

Figure 2. Flowchart of the phases of the aligning process.

3.1 Alignment of short arm with long arm

After the mechanical assembly of all the main structural parts (chambers, arms, detector and source towers) the first step is a preliminary definition of the angles between the two arms. The two arms are considered as two lines each defined by two points. For the short arm the first point is the Source Point (SP) and the center of the flange connecting the short arm to the Optical Chamber (OC). For the long arm the two points are the Detector Point (DP) and the center of the flange connecting the Long Arm with the MM chamber. These 4 points must be in the line of sight of the used laser tracker CAM2 Vantage by Faro. The critical angle to set is the angle in XZ plane (see Figure 1 for the coordinate system) and it is adjusted manually moving the X-ray source assembly along the curved guide using screws for X-ray source Z translation (Figure 3).

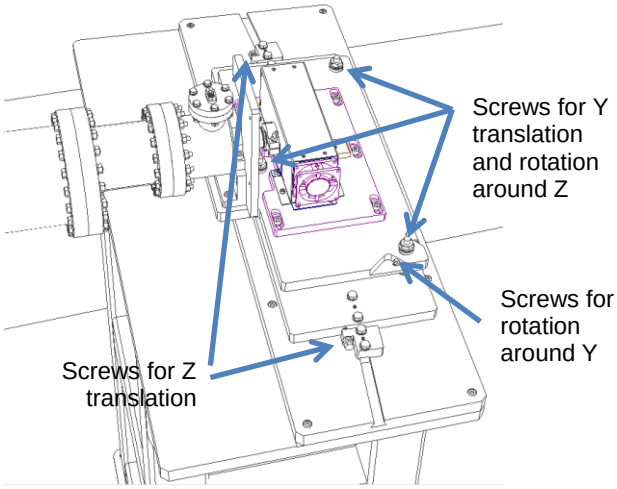

Figure 3. X-ray source tower with movements for alignment.

In this phase, the laser tracker is also used to check the bending of the arms and the parallelism to the floor foundations by acting on the screws for Y translation of the X-ray source and by acting on the motorization on which the CCD is mounted.

3.2 Alignment of X-ray source with reference plates

This alignment step is independent from the previous step, but is necessary to define with sufficient precision the position of the focal spot of the X-ray source. The theoretical position of the focal spot is known within 1 mm but a pinhole with a 0.4 mm diameter is mounted inside the KF16 interfacing flange to the Short Arm. The pinhole itself is precisely mounted and glued coaxial to the KF16 flange for:

1. identifying the nominal position of the source
2. limiting the aperture cone to about 6 degrees, the needed angle to cover all the parabolic mirror: in this way spurious reflection inside the Short Arm are avoided.

The position of the focal spot has to be referred to the reference plates that will be used in the next steps as reference feature with laser tracker measurements. To this end, the source assembly was dismounted from the source tower and measured with 3D coordinate machine (CMM). The measuring probe was able to enter inside the KF16 flange and to measure the corresponding center. The residual error in the determination of the focal spot position was refined in the next phase when the mirror was aligned to the X-ray source.

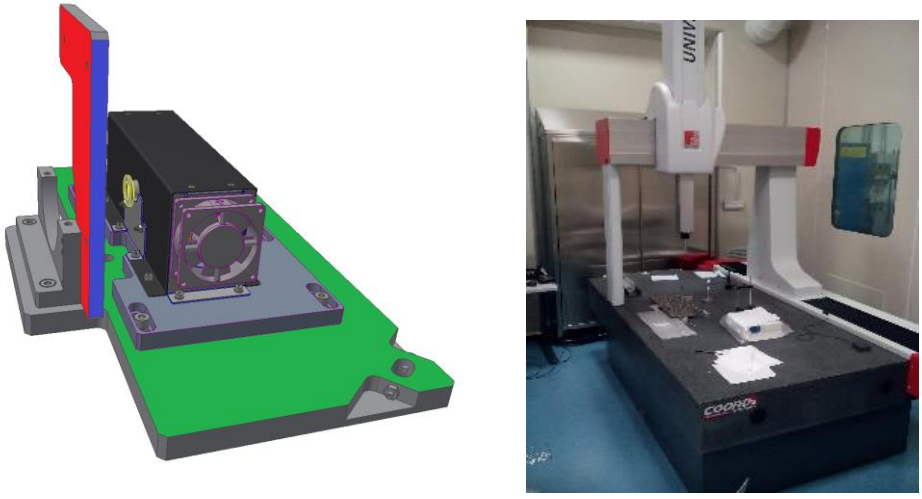

Figure 4. X-ray source assembly (left) mounted on 3D measuring machine (right) for the determination of the X-ray source position.

3.3 Alignment of X-ray source with short arm

The alignment of the different optical components proceeds along the direction of the photons path, therefore the first element to align is the X-ray source. The Short Arm (SA) is kept in vacuum and the X-ray source is switched on. At the end of SA a phosphor window, mounted in the interface with the Optical Chamber, converts the X-ray photons to visible light. The phosphor window also have the function to close the SA, which can be evacuated, while the Optical Chamber stays in air. A CCD, mounted outside the Optical chamber, detects the image of the phosphor created by a lens mounted in the OC (Figure 5). The X-ray Source rotation around Z and Y is then adjusted, by acting on screws (Figure 3) whose center of rotation is very near to the position of the X-ray source. In this way, negligible translations can occur.

Figure 5. Monitoring setup inside the Optical chamber to align the X-ray source to the SA (right). Visible image of the X-ray source, created on the phosphor window (left): the bright rings are the light scattered from the edges of the window, the uniform central circle is the direct light from the X-ray source after alignment.

3.4 Alignment of OC reference plate to X-ray source

The parabolic mirror is installed inside the OC on a reference plate, where the two channel cut crystals will also be mounted. It is mounted on two rotational stages (rotation around Y and Z), which have 0.5 arcsec resolution. The other degree of freedom of the parabolic mirror (rotation around X and the three translations) are not adjustable in vacuum and they must be fixed, before the installation into the chamber, with a 3D measuring machine. During this measurement, the nominal positions for the two motorized axes are also set.
At first, the reference plate is aligned with the Long Arm. To this end, a laser tracker is used to adjust the position of the OC reference plate, by manual adjustments and shimming, to align it to the Long Arm. Then, the X-ray source is aligned to the OC reference plate: as this is a critical alignment (the goal is to align the X-ray source within 100-200 μm), 2 different and complementary methods ("optical" and "mechanical" methods) were used, both to reduce the errors and to have a backup solution in the case one of the two methods would had failed.

- Optical method → Two virtual paths are defined on the reference plate by two pinholes and two crosshairs targets (Figure 6): these components are measured and aligned with a 3D machine. The virtual paths intersect at the source position. A laser, HRS015B @ 633 nm by Thorlabs, is mounted before the pinholes, and aligned to the first virtual path. The parabolic mirror reflects the laser light and it is aligned to reflect the laser spot to the intersection point of the two paths. A Micro Alignment Telescope (MAT) is mounted before the crosshairs, and it is used to define the intersection of the two virtual paths. The MAT can therefore image both the laser spot reflected by the parabolic mirror and pinhole present in front of the X-ray source. The source is aligned acting on the translation in Y and Z direction (screws in Figure 3), until the two images seen by the MAT superimpose.

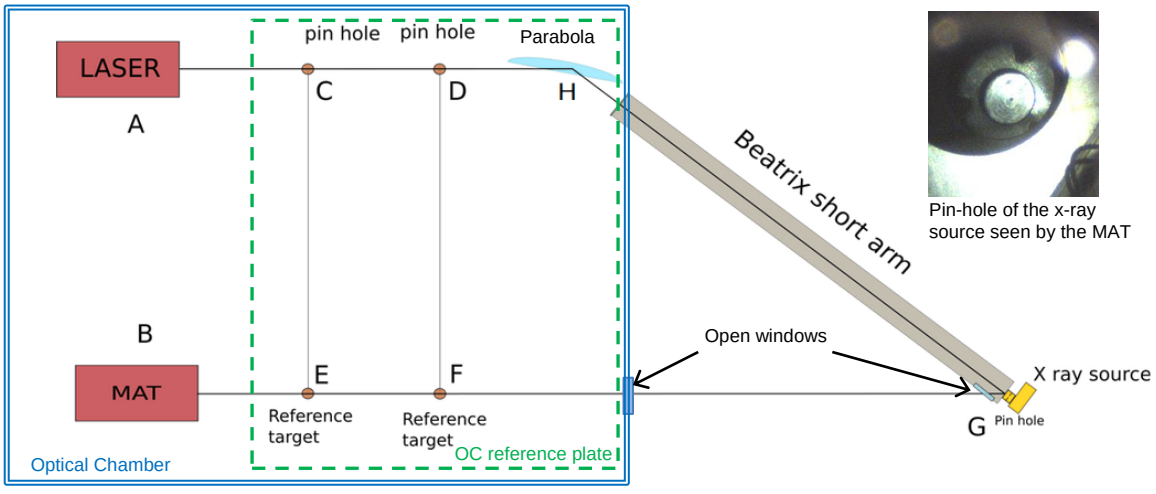

Figure 6. Sketch of the "optical" method to align position of the x-ray source

- Mechanical method → Once the parabolic mirror is aligned to the OC reference plate with the 3D measuring machine, selected features of the reference plate are also measured. After the OC reference plate is installed in the OC, a laser tracker is used to measure these features and refer them to other features of the plates of the X-ray-source, also pre-measured with the 3D machine.

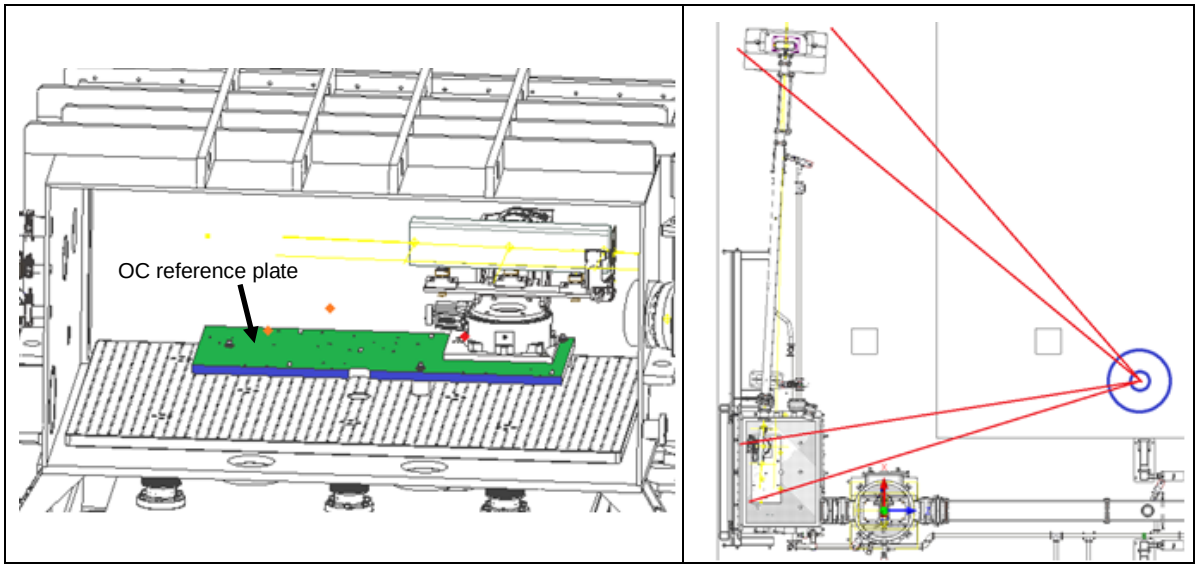

Figure 7. Features of the reference plate in the Optical Chamber used for measuring with laser tracker (left) and previously characterize under 3D measuring machine. Position of laser-tracker during alignment of X-ray source to the reference plate (right)

3.5 Alignment of mirror with OC reference plate and reference axes

The step described in the previous section is based on a precise characterization of the parabolic mirror w.r.t the OC reference plate. This precise characterization, done with 3D measuring machine, is necessary not only for the mirror itself, but also for the two axes described in section 3.4. The measured assembly is shown in Figure 8. In order to achieve an alignment of the X-ray source within 100-200 μm to OC reference plate, the accuracy of the position knowledge of the components, measured with the 3D measuring machine, must be less than 5 μm: in fact, the small distance between pinholes and crosshairs, compared with the mirror to X-ray source distance, would amplify the errors of about a factor 10. The remaining margin considered is due to the uncertainties of the "optical" method.

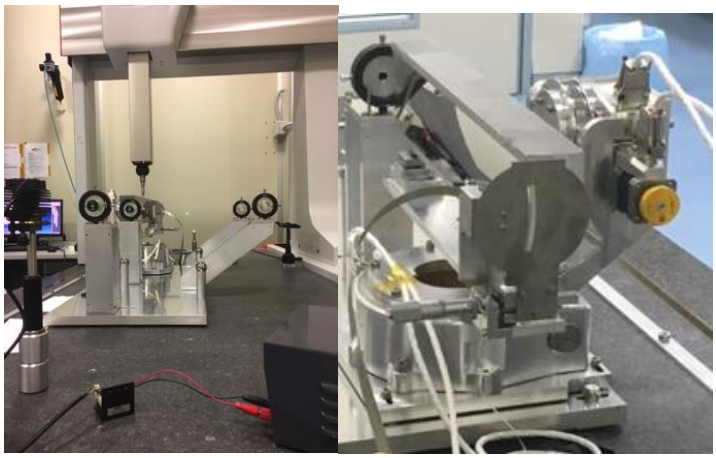

Figure 8. The OC reference plate with the parabolic mirror, pinholes and crosshair targets installed for the 3D measurements (left). Close look at the slit mounted and aligned in front of the mirror (right)

In order to reach this precision, the pinholes and crosshair targets have been characterized in details, defining their center w.r.t. the outer cylindrical surface. The 3D machine was used to measure the outer cylindrical surfaces, while the center of the pinholes and crosshairs was measured with the MAT in combination with the 3D machine (Figure 9).

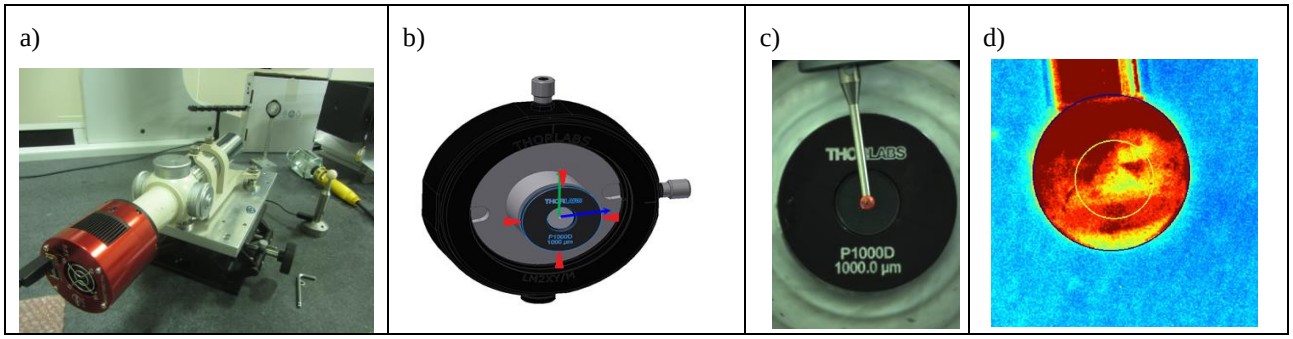

Figure 9. Procedure used to find the correct position of the center of the pinholes (or crosshair) with the 3D measuring machine: the MAT has been aligned perpendicular to the pinhole (or crosshair) (a), the outer cylindrical surface of the pinhole (or crosshair) is measured with the probe of the 3D machine to find the nominal center (b), two images are recorded with MAT, one without and one with the probe positioned just in front of the pinhole (or crosshair) (c), the image processing computed the real center (d).

In this phase, a slit was also mounted in front of the parabolic mirror and accurately aligned (*Figure 8*).
The measured error of the angle between the two virtual paths was 3 arcsec,

3.6 Alignment of mirror with X-ray source

After the procedure described in the previous sections, the X-ray source is pre-aligned to the parabolic mirror: in particular, the source is now fixed in term of translations and rotations, while the parabola is fixed only in the translations. The rotations of the mirror, only pre-aligned, are refined with a Hartmann test. A Hartmann plate is mounted just after the mirror (Figure 10). It is a stainless steel plate with an array of 400 µm-wide square holes, with a 250 µm thickness. The center-to-center hole spacing is 4 mm vertical and 2 mm horizontal. The holes are imaged on a CCD, mounted at the end of the Optical Chamber. As the CCD size is 27mm and the height of the beam is 60mm, only the central part of the beam is detected; this is anyway sufficient to adjust the rotations around Y (pitch) and around Z (yaw). In Figure 11 an example of the image is presented. The barycenter of each holes is computed: the result of the processing analysis is a map of the divergence interpolated between the squared holes. The 50% of the divergence is used as merit function for the optimization (Figure 12). Starting from 13 arcsec the reached divergence was 2 arcsec (Figure 11) in the central 25 × 4 mm.
At the end of this alignment, the Hartmann plate was dismounted, and the crystals positioned in the beam path.

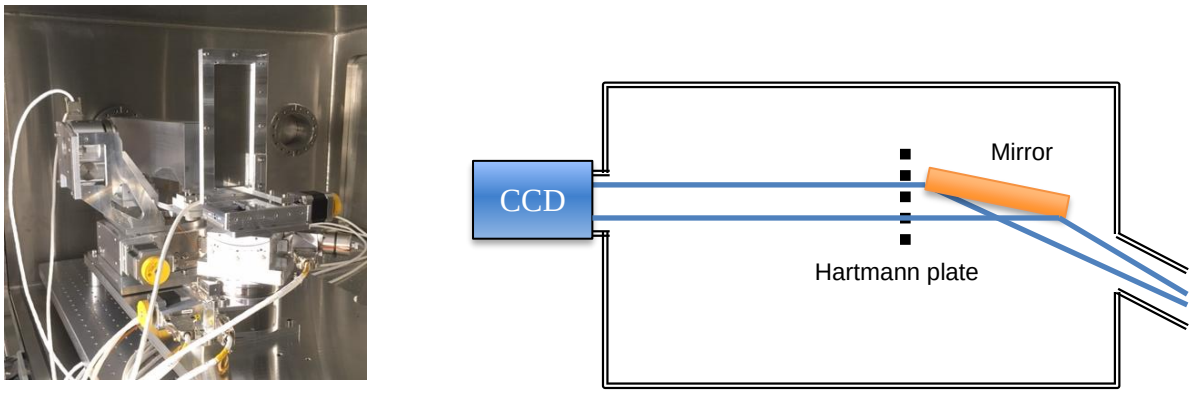

Figure 10. Hartmann plate mounted after the parabolic mirror. It is mounted on top of the motorization of the CCC1 (left). Sketch of the used setup (right).

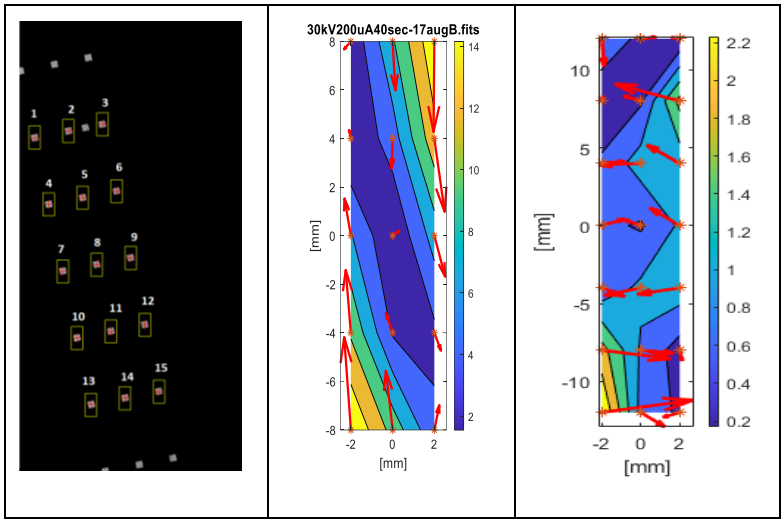

Figure 11. CCD image showing the holes of the Hartmann plate (left). The result of the alignment in term of divergence, comparing the starting (center) and the final result (right): the color map is expressed in arcsec. The red vectors represent the divergence of the corresponding holes

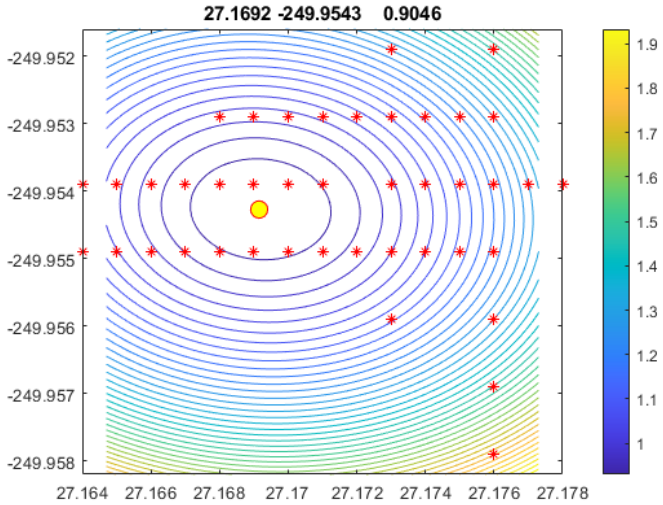

Figure 12. 50% of the total divergence plotted as function of yaw (X) and pitch (Y) of the parabolic mirror. The colored contours are in arcsec. The red dots are the measured positions

3.7 Alignment of CCC1 with X-ray beam

At first, only one channel cut crystal (CCC1) was mounted and aligned. It is mounted on its motorization assembly, composed by one translation stage to move the crystal in and out from the beam along Z, one rotational stage around Y to adjust the pitch and a cradle to adjust the roll. The alignment was reached using the detected flux as the merit function. This was measured with the CCD, flanged on the OC as for the parabolic mirror alignment (previous section).
The flux is very sensitive to the crystal pitch while it is not to the roll.

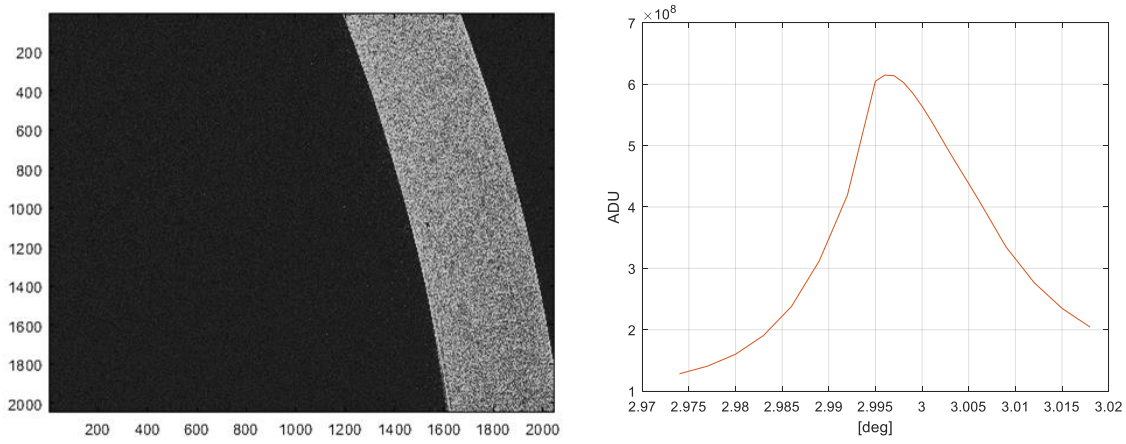

Figure 13. Image of the parallel beam after CCC1 (left). Flux detected with CCD as function of the crystal pitch (right) expressed in Analogic Digital Unit (ADU)

3.8 Alignment of CCC2 to X-ray beam

The alignment of CCC2 is very similar to the alignment of CCC1. The flux is monitored, but in this phase the not-uniformity of the beam assumes an important role. It is essentially a vertical variation of the intensity described by a second order polynomial law (Figure 14). It is caused by the small deviation of the mirror yaw from its nominal value. As CCC1, also in this case the critical adjustment is the pitch (Figure 15).

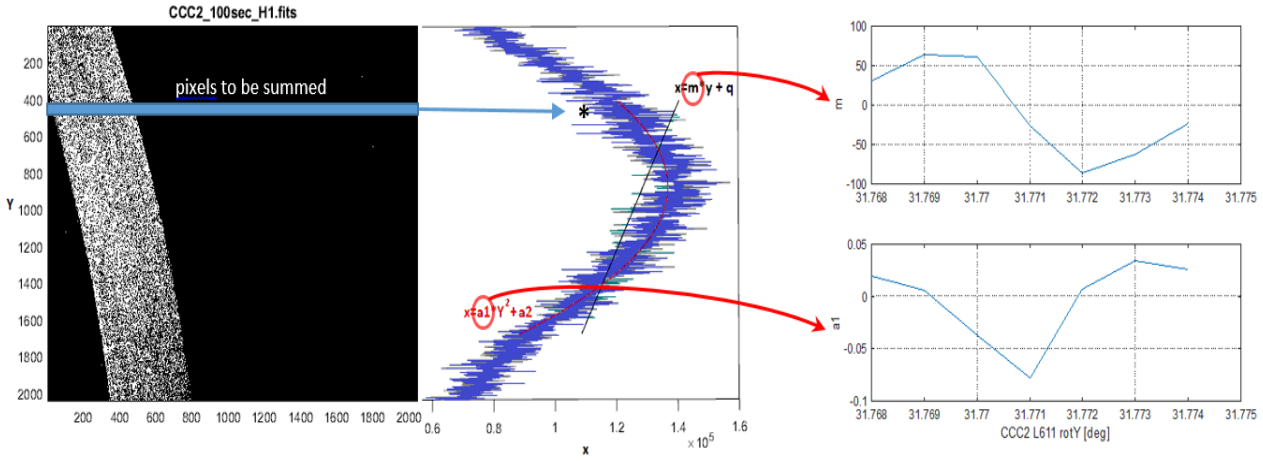

Figure 14. Image of the parallel beam after CCC2 (left) and description of the procedure for uniformity computation. Optimization of the CCC2 pitch (right)

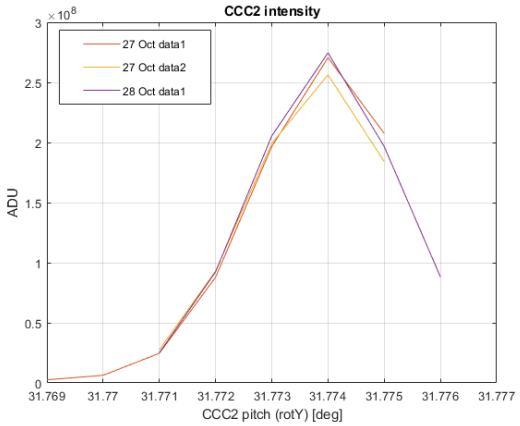

Figure 15. CCC2 pitch adjustment, maximizing the flux

3.9 Alignment of Beam Expander to X-ray beam

In the Optical Chamber the last optical element is the beam expander. It is mounted outside the reference frame on three motorizations: one translation stage along Z to center the crystal in the beam, one rotational stage around Y to adjust the pitch and a cradle to adjust the roll. The optimization is done with BE pitch looking the intensity of the flux. In this case is not possible to use the CCD mounted on the end of the chamber (as in Figure 10) because the beam is intercepted and 90 degrees deviated from the asymmetrically cut crystal. To measure the flux a beam monitor is mounted inside the chamber (Figure 16). The intensity curve in this case is broader than the same curves of the CCCs showing this alignment is not critical. The effect of the roll adjustment is essentially a deviation of the beam in vertical. This behavior can be exploit to bend the beam in the long arm upwards or downwards.

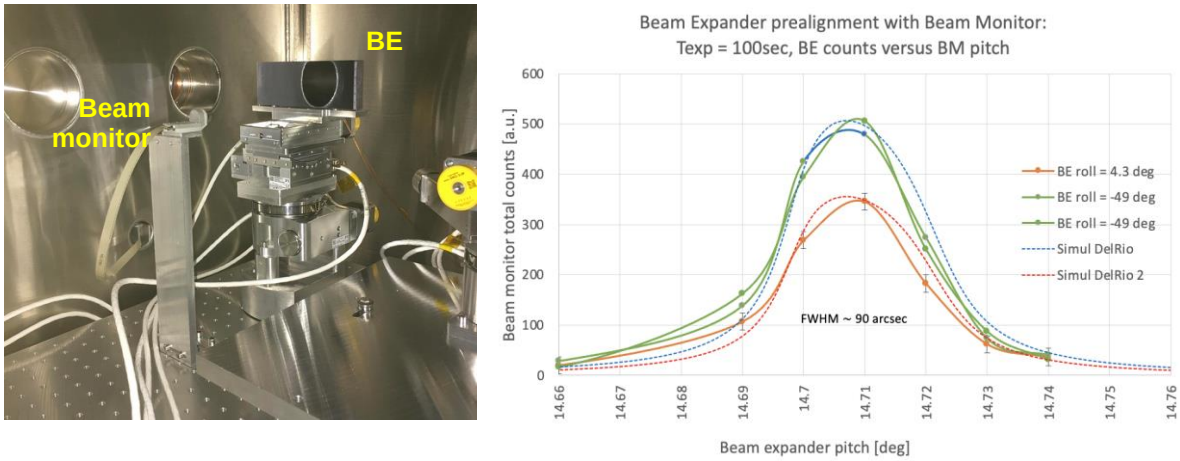

Figure 16. Beam Expander and beam monitor mounted in the Optical Chamber (left) and optimization of BE pitch (right)

The final step is the CCD mounting in the nominal position at the end of the Long Arm at 13m distance from the BE. In order to ease the individuation of the beam the Hartmann plate is mounted in the MM chamber.

4. CHARACTERIZATION OF THE BEAM

The X-ray beam size is 170 mm × 60 mm and the CCD size is 27 mm × 27 mm with an efficiency at the 4.51 keV of 60%. The entire parallel beam can be characterize only making a mosaic of 7 × 3 images. The mosaic is automatically

acquired by software[21], but the required time is long: each image is a sum of 18 frames for a total time of 1 hour, considering also the acquisition of the dark frames. The total time for a mosaic is 21 hours.
The mosaic can be acquired with or without the Hartmann plate (HP): the direct image of the beam without the Hartmann plate can be used to define the shape of the edges of the rectangular beam or to see the high frequency variation in term of flux. Placing HP in the MM chamber is useful to characterize the divergence and the flux uniformity in a low frequency range. The divergence in vertical direction (the main direction for the tests on the MMs) is 1.65 arcsec, considering all the possible contribution. The divergence in horizontal direction is worst: it is possible to choose a configuration with a better horizontal divergence, but low flux (2.7 arcsec and 10 ph/s/cm^2) or a configuration with a worst horizontal divergence and a high flux (3.45 arcsec and 60 ph/s/cm^2). The details of the procedure for the divergence computation is described in Ref. [20]. Concerning the low frequency uniformity, this is an information coming from the mosaic with the HP because in each of the 21 images is visible a dark region and it is possible to subtract the background in the correct way. This is not possible with an image completely lightened from the beam in the case of the mosaic without the HP. The obtained flux uniformity is in the order of 10% (Figure 17).

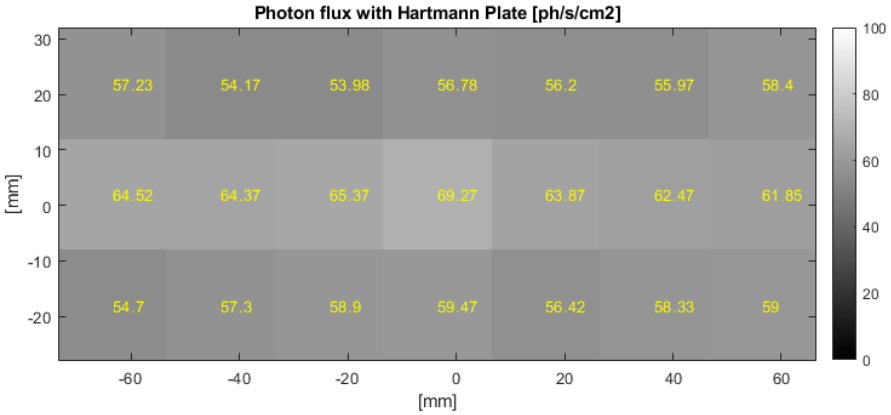

Figure 17. Beam flux of the parallel X-ray beam

5. CONCLUSION

The alignment procedure was a complex and long phase of the BEaTriX commissioning[22] involving different instruments and several ad-hoc setups, which required constrains on the design of the facility. An X-ray beam in line with the expectations was obtained[23]. The lessons learnt can be used in future for the second beam line (1.49 keV) to improve and also ease the alignment procedures.
The first line of BEaTriX (4.51 keV) is now working since early 2022. In the next months, the stability of the beam will be assessed in order to understand the time frequency for calibrations and re-alignments. Preliminary results indicate that the beam is stable for a time of the order of days if the facilities is on and the temperature is kept within 0.5 °C; if this conditions are satisfied, only a refinement of the pitch for the CCCs is needed daily.

REFERENCES

[1] Nandra, K., Barret, D., Barcons, X., et al., "The Hot and Energetic Universe: A White Paper presenting the science theme motivating the Athena mission," http://arxiv.org/abs/1306.2307 (2013).
[2] Bavdaz, M., Wille, E., Ayre, M., et al., "The ATHENA X-ray optics development and accomodation", Proc. SPIE 11852, 1185220 (2021)
[3] Collon, M. J., Babic, L., Barrière, N. M., et al. 2021, "X-ray mirror development and production for the ATHENA telescope", Proc. SPIE 11852, 118521Z (2021)
[4] Bradshaw, M., Burwitz, V, Hartner, G., et al., "Testing ATHENA optics: a new measurement standard at the PANTER x-ray test facility", Proc. SPIE 11852, 1185223 (2021)

[5] Menz, B., Braig, C., Br auninger, H., et al., “Large area x-ray collimator—the zone plate approach”, Applied Optics Vol. 54, Issue 26, pp. 7851-7858 (2015)
[6] Handick, E., Cibik, L. Krumrey, M., “Upgrade of the X-ray parallel beam facility XPBF 2.0 for characterization of silicon pore optics”, Proc. SPIE 11444, 114444G (2020)
[7] Spiga, D., Pareschi, G., Pelliciari, C., et al., “Functional tests of modular elements of segmented optics for x-ray telescopes via an expanded beam facility,” Proc. SPIE 8443, 84435F (2012)
[8] Spiga, D., Pelliciari, C., Bonnini, E., et al., "An expanded x-ray beam facility (BEaTriX) to test the modular elements of the ATHENA optics," Proc. SPIE 9144, 91445I (2014)
[9] Pelliciari, C., Spiga, D., Bonnini, E., et al., “BEaTriX, expanded soft x-ray beam facility for test of focusing optics, an update,” Proc. SPIE 9603, 96031P (2015)
[10] Spiga, D., Pelliciari, C., Salmaso, B., et al. “Design and advancement status of the Beam Expander Testing Xray facility (BEaTriX),” Proc. SPIE 9963, 996304 (2016)
[11] Salmaso, B., Spiga, D., Basso. S., et al., “Progress in the realization of the beam expander testing x-ray facility (BEaTriX) for testing ATHENA’s SPO modules,” Proc. SPIE 10699, 1069931 (2018)
[12] Spiga, D., Salmaso, B., Basso, S., et al, “Optical simulations for the laboratory-based expanded and collimated x-ray beam facility BEaTriX,” Proc. SPIE 11110, 111100E (2019)
[13] Basso, B., et al. Thermal simulations for characterization of ATHENA Mirror Modules with a radiating box in the BEaTriX facility, Proc. SPIE 111191, 111191I (2019)
[14] Salmaso, B., Spiga, D., Basso. S., et al., “BEaTriX (Beam Expander Testing X-ray facility) for testing ATHENA’s SPO modules: advancement status,” Proc. SPIE International Conference on Space Optics 2018, Vol. 11180, 1118026 (2019)
[15] Salmaso, B., et al. BEaTriX, the Beam Expander Testing X-ray facility for testing ATHENAs SPO modules: progress in the realisation, Proc. SPIE 11119, 111190N (2019)
[16] Ferrari, C., Beretta, S., Salmaso, B.,et al., “Characterization of ADP crystals for soft x-ray optics of the Beam Expander Testing X-ray facility (BEaTriX),” Journal of Applied Crystallography, 52, 599-604 (2019)
[17] Spiga D., Salmaso, B., Basso, S., et al., “Performance simulations for the ground-based, expanded-beam X-ray source BEaTriX”, Proc. SPIE 11837, 118370O (2021)
[18] Vecchi, G., Cotroneo, V., Ghigo, M., et al., Manufacturing and testing of the X-ray collimating mirror for the BEaTriX facility, Proc. SPIE 11822, 118220N (2021)
[19] Salmaso, B., Basso, S, Cotroneo, V. et al. “Building the BEaTriX facility for the ATHENA mirror modules X-ray testing”, Proc. SPIE 11822, 118220M (2021)
[20] Salmaso, B., Basso, S., Ghigo, M., et al.,“ X-ray tests of the ATHENA mirror modules in BEaTriX: from design to reality”, Proc. SPIE this conference
[21] Ghigo, M., Salmaso, B., Basso, S., et al., “The control software of the BEaTriX X-ray beam calibration facility: problems and solutions” , Proc. SPIE this conference
[22] Basso, S., Salmaso, B., Spiga, D., et al., “First light of BEaTriX, the new testing facility for the modular X-ray optics of the ATHENA mission”, Astronomy and Astrophysics, submitted
[23] Spiga, D., Salmaso, B., Basso, S., et al., “Optical design and performance simulations for the 1.49 keV beamline of the BEaTriX X-ray facility”, Proc. SPIE this conference